

Data-Driven Upper Bounds on Channel Capacity

Christian Häger, *Member, IEEE* and Erik Agrell, *Fellow, IEEE*

Abstract—We consider the problem of estimating an upper bound on the capacity of a memoryless channel with unknown channel law and continuous output alphabet. A novel data-driven algorithm is proposed that exploits the dual representation of capacity where the maximization over the input distribution is replaced with a minimization over a reference distribution on the channel output. To efficiently compute the required divergence maximization between the conditional channel and the reference distribution, we use a modified mutual information neural estimator that takes the channel input as an additional parameter. We evaluate our approach on different memoryless channels and show that the estimated upper bounds closely converge either to the channel capacity or to best-known lower bounds.

Index Terms—Autoencoders, channel capacity, divergence estimation, duality, dual capacity representation, mutual information neural estimation, neural networks, upper capacity bounds.

I. INTRODUCTION

The capacity of a communication channel is the maximum rate that can be reliably transmitted [1]. Even though capacity is of fundamental importance for both theory and practice, exact analytical expressions are only available in relatively few cases. If the underlying channel law is known, numerical techniques can be used to approximately compute capacity such as the well-known Blahut–Arimoto algorithm [2], [3] and its many variations, see, e.g., [4] and references therein.

Recently, there has been significant interest in developing capacity estimation algorithms based on machine learning, without assuming knowledge about the underlying channel law [5]–[11]. These approaches have their origin in the seminal work [12], where the authors propose to reinterpret the communication problem as a reconstruction task using parameterized transmitters and receivers, similar to autoencoders (AEs) in machine learning. It can be shown that the cross-entropy minimization commonly used to train AEs maximizes a lower bound on mutual information, whereas the transmitter optimization can be regarded as shaping a discrete input distribution. Using this approach, tight lower bounds on the capacity of a nonlinear phase noise (NLPN) channel were for example obtained in [5].

A disadvantage of the AE approach is that it requires a differentiable channel model to compute gradients for the transmitter optimization. Therefore, it cannot be used directly in practical settings where the channel is only accessible via

This work was supported by the Knut and Alice Wallenberg Foundation (grant no. 2018.0090) and the Swedish Research Council (grants no. 2020-04718 and 2021-03709). The computations were enabled by resources provided by the Swedish National Infrastructure for Computing (SNIC) at the Chalmers Centre for Computational Science and Engineering (C3SE) partially funded by the Swedish Research Council (grant no. 2018-05973).

C. Häger and E. Agrell are with the Department of Electrical Engineering, Chalmers University of Technology, 41296 Gothenburg, Sweden (email: {hagerc, agrell}@chalmers.se).

input–output samples. To address this problem, [6] proposes to use the sample-based mutual information neural estimation (MINE) technique from [13] and train the AE transmitter based on the (differentiable) MINE. Related approaches were subsequently proposed for feedback channels with memory¹ in [7] and for memoryless multiple-access channels in [9]. Moreover, a hybrid approach that regularizes the cross-entropy-based AE training using MINE is proposed in [10]. Comparisons of various sample-based mutual information estimators similar to MINE can be found in [8] and [11].

All of the above learning-based approaches target the estimation of *lower* capacity bounds using the conventional maximization of mutual information (or directed information in [7]) over the input distribution, see (1) below. In this paper, we follow a different path and consider the problem of estimating an *upper* capacity bound by exploiting the dual representation of channel capacity, which is described in Sec. II. Our work relies on a variation of MINE for estimating the divergence between the conditional channel and a given reference distribution. The resulting method can be applied to memoryless channels with a continuous output alphabet. Similar to [5]–[11], it is agnostic to the underlying channel law.

Notation: Random variables are denoted by upper-case letters (e.g., X), realizations by lower-case letters (e.g., x), and sets by calligraphic letters (e.g., \mathcal{X}). The probability distribution of a random variable X is denoted by f_X . $\mathbb{E}[\cdot]$ denotes expectation, $I(\cdot; \cdot)$ mutual information, and $D(\cdot \parallel \cdot)$ Kullback–Leibler divergence. For an integer N , we define the set $[N] = \{1, 2, \dots, N\}$.

II. DUAL REPRESENTATION OF CHANNEL CAPACITY

We consider a memoryless channel with input $X \in \mathcal{X}$ and output $Y \in \mathcal{Y}$.² The channel law conditioned on a particular input x is denoted by $f_{Y|X=x}(y)$. In general, the input is assumed to be constrained by a cost function $c: \mathcal{X} \rightarrow \mathbb{R}_{\geq 0}$. The application of c to an input distribution f_X is defined by $c(f_X) = \mathbb{E}_{f_X}[c(X)]$ [15, p. 108]. The capacity of such a channel is

$$C = \max_{f_X: c(f_X) \leq P} I(X; Y), \quad (1)$$

where P denotes the maximum average cost. In the following, we work with the dual representation [15, p. 142]

$$C = \min_{\gamma \geq 0} [F(\gamma) + \gamma P], \quad (2)$$

¹See also the earlier work in [14] based on reinforcement learning, which, however, requires knowledge about the channel law.

²To keep the notation simple, we focus on scalar channels. However, our approach generalizes to (block-wise) memoryless channels where the input and outputs are (possibly complex-valued) random vectors, see Sec. VI-C.

where

$$F(\gamma) = \min_{q_Y} \max_{x \in \mathcal{X}} [D(f_{Y|X=x} || q_Y) - \gamma c(x)]. \quad (3)$$

The minimization in (3) is over all distributions q_Y on \mathcal{Y} . Note that any fixed choice for the reference distribution q_Y leads to an upper bound in (3) and hence on the capacity (2).

According to [16], the above dual approach first originated in [17] and was further developed in [18], [15], and [19]. Recent work exploiting this approach has mostly focused on choosing q_Y to obtain a tractable analytical expression for the resulting upper bound, see, e.g., [16], [19]. In this paper, we will instead use (3) as a blueprint for an iterative optimization procedure that alternates between training a divergence estimator (see Sec. III) and the reference distribution q_Y (see Sec. IV) based on the obtained estimator. The resulting algorithm is described in Sec. V.

III. DATA-DRIVEN DIVERGENCE ESTIMATION

We use the approach proposed in [13] to estimate the divergence term in (3). This approach is based on the Donsker–Varadhan representation [13, Th. 1]

$$D(f_{Y|X=x} || q_Y) = \sup_{T \in \mathcal{T}} \mathbb{E}_{f_{Y|X=x}} [T(Y)] - \log \left(\mathbb{E}_{q_Y} \left[e^{T(Y)} \right] \right), \quad (4)$$

where the supremum is over all functions $T : \mathcal{Y} \rightarrow \mathbb{R}$ such that the expectations in (4) are finite. The idea in [13] is to approximate the class of functions \mathcal{T} using a neural network (NN) $T_\theta : \mathcal{Y} \rightarrow \mathbb{R}$, where θ are the NN parameters. T_θ is also referred to as the statistics network. For a fixed set of parameters θ , the resulting estimator is

$$\hat{D}_\theta = \frac{1}{B} \sum_{i=1}^B T_\theta(y^{(i)}) - \log \left(\frac{1}{B} \sum_{i=1}^B e^{T_\theta(\tilde{y}^{(i)})} \right), \quad (5)$$

where B is the batch size, $y^{(1)}, \dots, y^{(B)} \sim f_{Y|X=x}$, and $\tilde{y}^{(1)}, \dots, \tilde{y}^{(B)} \sim q_Y$. This estimator can be iteratively trained by running gradient ascent on (5), see [13, Alg. 1] for details.

Remark. We use the above estimator mainly for its simplicity and the fact that it empirically tends to work well (see, e.g., [11]). However, one should be aware of its limitations, e.g., the gradients resulting from (5) are biased [13], the estimator has high variance, especially if the true underlying divergence is large [20], and it provides neither a guaranteed upper nor lower bound on divergence for a finite sample size [21]. We comment on potential alternative approaches in Sec. VII.

Note that the estimator (5) assumes a fixed channel input x . A different statistics network T_θ would thus be required for each input to evaluate the maximization in (3) over the input alphabet. However, this quickly becomes infeasible if the size of the input alphabet is large or infinite. To circumvent this problem, we propose a modified version of (5) where the input x is taken as an additional input to the statistics network T_θ , i.e., $T_\theta : \mathcal{Y} \times \mathcal{X} \rightarrow \mathbb{R}$. The resulting modified estimator is denoted by

$$\hat{D}_\theta(x) = \frac{1}{B} \sum_{i=1}^B T_\theta(y^{(i)}, x) - \log \left(\frac{1}{B} \sum_{i=1}^B e^{T_\theta(\tilde{y}^{(i)}, x)} \right). \quad (6)$$

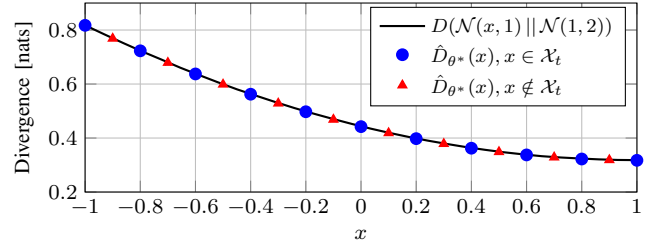


Fig. 1: Accuracy and generalization ability of the trained divergence estimator (6), where $\mathcal{X}_t = \{-1, -0.8, \dots, +1\}$.

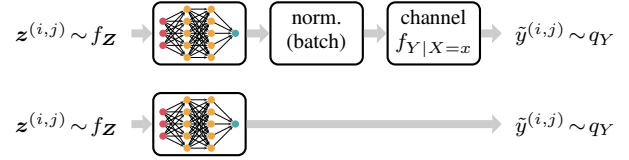


Fig. 2: Two approaches for implementing the neural distribution transformer (NDT) that generates samples from the reference distribution q_Y .

This formulation allows us to train a single statistics network that works well for a range of different channel inputs. In particular, this can be accomplished by jointly considering multiple inputs $\{x^{(1)}, \dots, x^{(N_t)}\} = \mathcal{X}_t \subseteq \mathcal{X}$ and running gradient descent on an average loss defined by

$$\begin{aligned} L_\theta &= -\frac{1}{N_t} \sum_{j=1}^{N_t} \hat{D}_\theta(x^{(j)}) \\ &= -\frac{1}{N_t} \sum_{j=1}^{N_t} \left[\frac{1}{B} \sum_{i=1}^B T_\theta(y^{(i,j)}, x^{(j)}) \right. \\ &\quad \left. - \log \left(\frac{1}{B} \sum_{i=1}^B e^{T_\theta(\tilde{y}^{(i,j)}, x^{(j)})} \right) \right], \end{aligned} \quad (7)$$

where $y^{(1,j)}, \dots, y^{(B,j)} \sim f_{Y|X=x^{(j)}}$ and $\tilde{y}^{(1,j)}, \dots, \tilde{y}^{(B,j)} \sim q_Y$.

Example: Assume that $f_{Y|X=x}$ and q_Y correspond to $\mathcal{N}(x, 1)$ and $\mathcal{N}(1, 2)$, respectively. To optimize the parameters θ , we set $\mathcal{X}_t = \{-1, -0.8, \dots, +1\}$ and train the statistics network³ using the average loss (7). Fig. 1 compares the accuracy of the resulting estimator $\hat{D}_{\theta^*}(x)$ to the true divergence as a function of x , where θ^* refers to the optimized parameters. Note that $\hat{D}_{\theta^*}(x)$ generalizes well even to values of x that were not seen during training, as illustrated by the red triangles. \triangle

IV. REPRESENTATION OF THE REFERENCE DISTRIBUTION

To allow for the gradient-based optimization of the reference distribution q_Y , two different approaches are described in the following for generating the samples $\tilde{y}^{(1,j)}, \dots, \tilde{y}^{(B,j)} \sim q_Y$ in (7) using NNs. The corresponding block diagrams are shown in Fig. 2. Similar to [7], we refer to the resulting transformation as the neural distribution transformer (NDT).

In the first approach (Fig. 2, top), the NDT consists of an NN f_τ with parameters τ , which is then followed by a batch-wise normalization procedure and transmission over the

³The NN architecture and all other training hyperparameters for this example are the same as for case (i) in Tabs. I and II below.

channel. In particular, the normalization procedure enforces the average cost constraint⁴ via

$$\tilde{s}^{(i,j)} = \frac{s^{(i,j)}}{c^{-1} \left(\frac{1}{B} \sum_{i=1}^B c(s^{(i,j)}) \right)}, \quad (8)$$

where $s^{(i,j)} = f_\tau(\mathbf{z}^{(i,j)})$, $i \in [B]$, $j \in [N_i]$ is the NN output and $\mathbf{z}^{(i,j)} \in \mathbb{R}^l$ is a random vector sampled from a fixed latent probability distribution $f_{\mathbf{Z}}$. Note that (8) implicitly assumes that the cost function distributes over division, i.e., $c(a/b) = c(a)/c(b)$, which is the case for all cost functions considered in this paper. The above approach ensures that q_Y is a valid output distribution for the channel under consideration, given the cost constraint. However, it should be noted that it requires a differentiable channel model in order to compute gradients with respect to τ .

In the second approach (Fig. 2, bottom), the NDT simply consists of an NN f_τ as before but without any additional post-processing, i.e., $\tilde{y}^{(i,j)} = f_\tau(\mathbf{z}^{(i,j)})$. While this approach does not necessarily ensure that q_Y is a valid output distribution for cost-constrained channels (which is not required to obtain an upper bound in (3)), it is more universal and can be used even if the channel is only accessible as a black box through input–output samples (e.g., in an experimental setting). On the other hand, we found that this representation typically requires more training steps when optimizing the NN parameters τ .

V. PROPOSED ALGORITHM

The proposed capacity estimation algorithm is detailed in Algorithm 1. It alternates between training the statistics network T_θ (lines 3–5) and the NDT network f_τ (lines 6–8) for a total of \mathcal{I} iterations. The latter optimizes the reference distribution q_Y based on the loss function (cf. (3))

$$\begin{aligned} \hat{F}_\tau(\gamma) &= \max_{j \in [N_d]} \left[\hat{D}_\theta(x^{(j)}) - \gamma c(x^{(j)}) \right] \\ &= \max_{j \in [N_d]} \left[\frac{1}{B} \sum_{i=1}^B T_\theta(\tilde{y}^{(i,j)}, x^{(j)}) \right. \\ &\quad \left. - \log \left(\frac{1}{B} \sum_{i=1}^B e^{T_\theta(\tilde{y}^{(i,j)}, x^{(j)})} \right) - \gamma c(x^{(j)}) \right], \end{aligned} \quad (9)$$

where the dependence of $\hat{F}_\tau(\gamma)$ on the parameters τ is implicit through the samples $\tilde{y}^{(i,j)}$ generated by the NDT. Compared to (3), the outer minimization over q_Y is encapsulated in the NN parameters τ , which are optimized via gradient descent in Algorithm 1.

The definition of the sets \mathcal{X}_t and $\{x^{(1)}, \dots, x^{(N_d)}\} = \mathcal{X}_d \subseteq \mathcal{X}$ appearing in lines 3 and 6 depends on whether the channel input alphabet is discrete or continuous. For channels with discrete input alphabet \mathcal{X} , we may set $\mathcal{X}_t = \mathcal{X}_d = \mathcal{X}$.⁵ If the input alphabet of the channel is continuous, we assume that the input space has been appropriately discretized and the resulting set of discretized inputs is given by \mathcal{X}_d . To ensure that the capacity of the resulting input-discretized channel is close

⁴Note that this procedure enforces the average cost constraint with equality, even if the inequality constraint was satisfied before the normalization.

⁵In this case, the data generated in line 3 can be reused in line 6.

Algorithm 1: Estimation of capacity upper bounds.

1 Inputs: number of iterations \mathcal{I} , batch size B , learning rate β , Lagrange multiplier γ (for cost-constrained channels), input sets \mathcal{X}_t (see Sec. III) and \mathcal{X}_d (see Sec. V)

2 for $l = 1, 2, \dots, \mathcal{I}$ **do**

3 $\forall x^{(j)} \in \mathcal{X}_t, i \in [B]$: generate $y^{(i,j)} \sim f_{Y|X=x^{(j)}}$, $\tilde{y}^{(i,j)} \sim q_Y$

4 $L_\theta \leftarrow$ compute average loss according to (7)

5 $\theta \leftarrow \theta - \beta \nabla_\theta L_\theta$ /* update statistics network */

6 $\forall x^{(j)} \in \mathcal{X}_d, i \in [B]$: generate $y^{(i,j)} \sim f_{Y|X=x^{(j)}}$, $\tilde{y}^{(i,j)} \sim q_Y$

7 $\hat{F}_\tau(\gamma) \leftarrow$ estimate upper bound according to (9)

8 $\tau \leftarrow \tau - \beta \nabla_\tau \hat{F}_\tau(\gamma)$ /* update NDT network */

9 return $\hat{F}_\tau(\gamma)$

TABLE I: NN parameters for the (i) average-power-constrained AWGN, (ii) peak-power-constrained AWGN, (iii) OI, and (iv) NLPN channel.

	layer	NDT network f_τ			statistics network T_θ		
		input	hidden	output	input	hidden	output
(i)	# of layers	-	2	-	-	2	-
	# of neurons	50	100	1	2	100	1
	act. function	-	ReLU	linear	-	ReLU	linear
(ii)	# of layers	-	2	-	-	2	-
	# of neurons	50	100	1	2	100	1
	act. function	-	ReLU	tanh	-	ReLU	linear
(iii)	# of layers	-	2	-	-	2	-
	# of neurons	50	100	1	2	100	1
	act. function	-	ReLU	sigmoid	-	ReLU	linear
(iv)	# of layers	-	2	-	-	2	-
	# of neurons	50	150	2	4	150	1
	act. function	-	ReLU	linear	-	ReLU	linear

to that of the original channel, one approach is to successively increase the number of discretization points N_d until some form of convergence is reached. A native, but more involved, approach for channels with continuous inputs that does not require any input space discretization is suggested in Sec. VII.

VI. NUMERICAL RESULTS

In this section, we evaluate the proposed approach by estimating upper bounds on the capacity of various memoryless channels.⁶ Note that for cost-constrained channels, Algorithm 1 estimates the capacity in (3) as a function of the Lagrange multiplier $\gamma \geq 0$. In this case, we use a golden-section search to solve the outer one-dimensional minimization over γ in (2).

For all considered cases, we use fully-connected NNs with rectified linear unit (ReLU) activation functions in the hidden layers to represent both the NDT network f_τ and the statistics network T_θ . The NN parameters are summarized in Tab. I. The number of input neurons for f_τ depends on the latent distribution, which we assume to be a multivariate Gaussian distribution $\mathcal{N}(\mathbf{0}_l, \mathbf{I}_l)$ with $l = 50$. We found that the results are relatively insensitive to the choice of l , which mainly affects the initial distribution for q_Y before training. Moreover, while we have verified both NDT approaches discussed in Sec. IV, the following numerical results use the first approach (Fig. 2, top) since all channel models below are differentiable.

For the gradient-based optimization steps in Algorithm 1 (lines 5 and 8), we employ the Adam optimizer [22] with

⁶The source code to reproduce all numerical results in this paper is available at https://github.com/chaeger/upper_capacity_bounds.

TABLE II: Training parameters for the (i) average-power-constrained AWGN, (ii) peak-power-constrained AWGN, (iii) OI, and (iv) NLPN channel.

	(i)	(ii)	(iii)	(iv)
number of iterations \mathcal{I}	500	500	500	2500
batch size B	20000	20000	20000	20000
learning rate β	10^{-3}	10^{-3}	10^{-3}	10^{-3}
input discretization points N_d	15	15	15	81

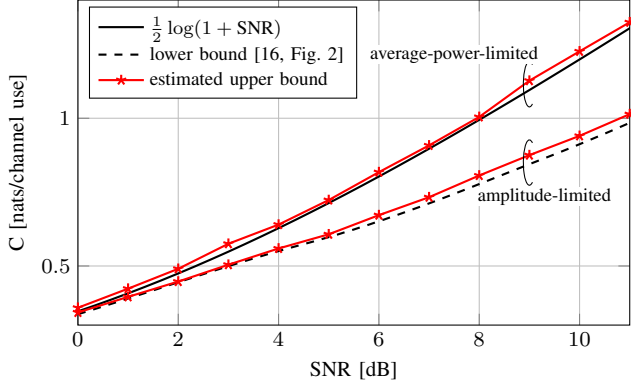


Fig. 3: Results for the AWGN channel.

learning rate and batch size shown in Tab. II. The table also shows the number of iterations and discretization points for each scenario. Lastly, we always pretrain the statistics network T_θ by running 200 initial iterations of lines 3–5 in Algorithms 1, which we found to improve training convergence.

A. AWGN Channel

We start with the additive white Gaussian noise (AWGN) channel $Y = X + Z$, where X is the channel input and $Z \sim \mathcal{N}(0, \sigma^2)$. For the average-power-limited case, we have $c(x) = x^2$ as a cost function, in which case $C = \frac{1}{2} \log(1 + \text{SNR})$ with $\text{SNR} = P/\sigma^2$. For the amplitude-limited case, we instead have no cost constraint, $|X| \leq A$, and $\text{SNR} = A^2/\sigma^2$. In this case, no closed-form analytical capacity expressions exist, but upper and lower bounds have been derived, see, e.g., [16], [23] and references therein.

For the numerical estimation, we set $P = 1$ and $A = 1$ without loss of generality and vary the SNR by varying σ^2 . The input space is discretized using $N_d = 15$ uniformly spaced grid points in the intervals $[-2.5, 2.5]$ and $[-1, 1]$ for the average-power-limited and amplitude-limited case, respectively. In this paper, we always assume for simplicity that $\mathcal{X}_t = \mathcal{X}_d$, noting that in general the set \mathcal{X}_d can be different from the set \mathcal{X}_t used to train the divergence estimator. Fig. 3 shows the estimated upper bounds, where we compare to the lower bound in [16, Fig. 2] for the amplitude-limited case. Note that the NDT network f_τ for the amplitude-limited case uses a tanh activation function in the last layer (cf. Tab. I) to enforce the amplitude constraint. Moreover, due to the absence of a cost constraint, no normalization procedure is applied and the outputs of f_τ are directly transmitted over the channel to generate the NDT output samples $\tilde{y}^{(i,j)}$.

B. Optical Intensity Channel

Next, we consider the optical intensity (OI) channel which is defined by $Y = X + Z$ with $c(x) = x$, $X \in [0, A]$, and

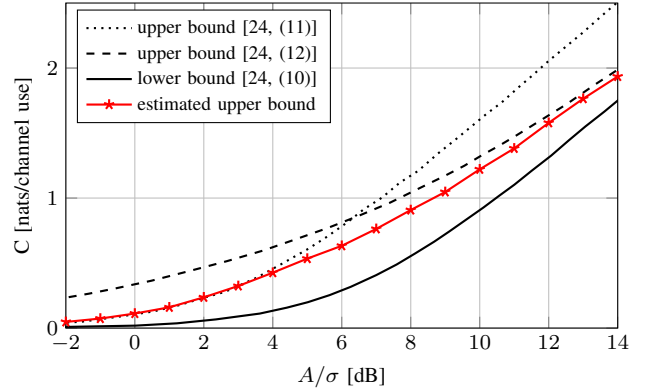


Fig. 4: Results for the OI channel with $\alpha = 0.4$ (cf. [24, Fig. 2])

$Z \sim \mathcal{N}(0, \sigma^2)$ [24]. We consider the case $\alpha = P/A = 0.4$. For the numerical estimation, we set $P = 1$ and discretize the input space using 15 uniformly spaced grid points in the interval $[0, A]$, where $A = 2.5$. For this case, the NDT network uses a sigmoid activation (scaled by A) in the last layer to ensure that the channel input satisfies the amplitude constraint. Results are shown in Fig. 4, where we compare to the upper and lower capacity bounds developed in [24], see in particular [24, Fig. 2]. The gap of the estimated upper bound with respect to the lower bound is due to the fact that the latter is not tight. Indeed, we used the Blahut–Arimoto algorithm for cost-constrained channels [15, p. 140] to verify that the channel capacity is close to our estimated upper bound.

C. Nonlinear Phase Noise Channel

Lastly, we consider an NLPN channel for coherent optical communication which is based on a split-step solution of the nonlinear Schrödinger equation without dispersive effects. The resulting complex-valued channel is defined by the recursion

$$X_{k+1} = X_k e^{j\gamma L |X_k|^2 / K} + N_{k+1}, \quad 0 \leq k \leq K, \quad (10)$$

where $X = X_0 \in \mathbb{C}$ is the input, $Y = X_K \in \mathbb{C}$ is the output, $N_{k+1} \sim \mathcal{CN}(0, \sigma^2/K)$, σ^2 is the total noise power, γ is a nonlinearity parameter, L is the transmission distance, and $c(x) = |x|^2$. This channel has a long history in terms of capacity analysis, see [5], [25] and references therein. Here, we use the same parameters as in [5], [25], i.e., $K = 50$, $\sigma^2 = -21.3$ dBm, $\gamma = 1.27$ rad/km/W, and $L = 5000$ km.

For the numerical estimation, we consider a renormalized version of (10), where $\tilde{X}_k = X_k/\sqrt{P}$. The input space of the renormalized channel is discretized using 9 uniformly spaced grid points in the interval $[-1.75, 1.75]$ for both the real and imaginary part, i.e., $N_d = 81$ total discretization points. Separating the real and imaginary parts of the channel input and output, respectively, the number of NDT output neurons is increased to 2 and the number of input neurons of the statistics network to 4. Fig. 5 shows the obtained results as a function of P (see the top axis for a conversion to $\text{SNR} = P/\sigma^2$). It can be seen that the estimated upper bound closely follows the lower bound in [25], which is based on a Gaussian input distribution.

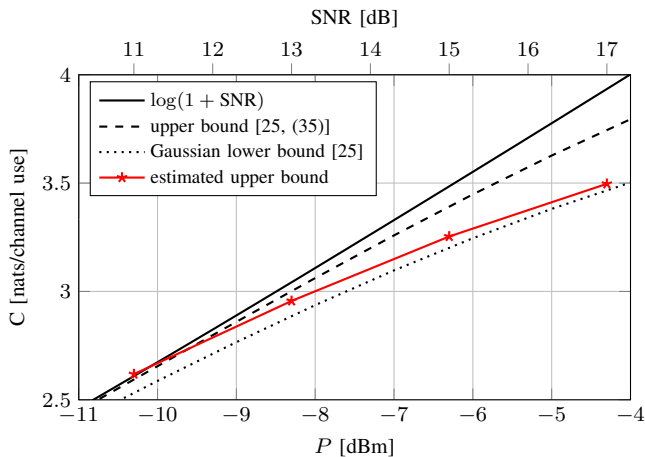


Fig. 5: Results for the NLPN channel.

VII. DISCUSSION AND FUTURE WORK

We have proposed a novel data-driven approach for estimating upper bounds on channel capacity. The approach exploits the dual representation of capacity and does not require knowledge about the underlying channel law. Similar to recent work in [6], [7], the proposed algorithm relies on the Donsker–Varadhan representation for estimating divergence, with the consequence that the resulting estimates are neither true upper nor lower bounds. An overview of potential alternative divergence estimation approaches can be found in [8] and [11]. Moreover, [9] recently proposed an approach to obtain outer bounds on the achievable rate region of memoryless multiple-access channels by exploiting the upper bounds based on f -divergence inequalities from [26]. However, the histogram-based approach to numerically evaluate these bound in [9] does not directly lead to a differentiable loss function. Therefore, additional modifications (e.g., based on ideas similar to [27]) would be required to be able to use such inequalities in conjunction with the NDT optimization in Algorithm 1.

Lastly, we have assumed that the input alphabet of the channel is either discrete or has been appropriately discretized. For future work, it may be interesting to develop native estimation approaches for continuous-input channels that do not require such a discretization. This could be done, for example, by considering an auxiliary distribution over the input space and casting the maximization in (3) as an optimization problem over this auxiliary distribution. Similar to the NDT, the auxiliary distribution could then again be parameterized using an NN.

REFERENCES

- [1] C. E. Shannon, “A mathematical theory of communication,” *Bell System Technical Journal*, vol. 27, pp. 379–423, Jul. 1948.
- [2] R. Blahut, “Computation of channel capacity and rate-distortion functions,” *IEEE Trans. Inf. Theory*, vol. 18, no. 4, pp. 460–473, Jul. 1972.
- [3] S. Arimoto, “An algorithm for computing the capacity of arbitrary discrete memoryless channels,” *IEEE Trans. Inf. Theory*, vol. 18, no. 1, pp. 14–20, Jan. 1972.
- [4] I. Naiss and H. H. Permuter, “Extension of the Blahut–Arimoto Algorithm for Maximizing Directed Information,” *IEEE Trans. Inf. Theory*, vol. 59, no. 1, pp. 204–222, Jan. 2013.
- [5] S. Li, C. Häger, N. Garcia, and H. Wymeersch, “Achievable Information Rates for Nonlinear Fiber Communication via End-to-end Autoencoder Learning,” in *Proc. European Conf. Optical Communication (ECOC)*, Rome, Italy, 2018.
- [6] R. Fritschek, R. F. Schaefer, and G. Wunder, “Deep Learning for Channel Coding via Neural Mutual Information Estimation,” in *Proc. IEEE Int. Workshop on Signal Processing Advances in Wireless Communications (SPAWC)*, Cannes, France, 2019.
- [7] Z. Aharoni, D. Tsur, Z. Goldfeld, and H. H. Permuter, “Capacity of Continuous Channels with Memory via Directed Information Neural Estimator,” in *Proc. IEEE Int. Symp. Information Theory (ISIT)*, Los Angeles, CA, 2020.
- [8] R. Fritschek, R. F. Schaefer, and G. Wunder, “Neural Mutual Information Estimation for Channel Coding: State-of-the-Art Estimators, Analysis, and Performance Comparison,” in *Proc. IEEE Int. Workshop on Signal Processing Advances in Wireless Communications (SPAWC)*, Atlanta, GA, 2020.
- [9] F. Mirkarimi and N. Farsad, “Neural Computation of Capacity Region of Memoryless Multiple Access Channels,” in *Proc. IEEE Int. Symp. Information Theory (ISIT)*, Melbourne, Australia, 2021.
- [10] N. A. Letizia and A. M. Tonello, “Capacity-Driven Autoencoders for Communications,” *IEEE Open J. Commun. Soc.*, vol. 2, pp. 1366–1378, Jun. 2021.
- [11] F. Mirkarimi, S. Rini, and N. Farsad, “Neural Capacity Estimators: How Reliable Are They?” *arXiv:2111.07401 [cs.IT]*, Nov. 2021.
- [12] T. O’Shea and J. Hoydis, “An Introduction to Deep Learning for the Physical Layer,” *IEEE Trans. Cogn. Commun. Netw.*, vol. 3, no. 4, pp. 563–575, Dec. 2017.
- [13] M. I. Belghazi, A. Baratin, S. Rajeswar, S. Ozair, Y. Bengio, A. Courville, and R. D. Hjelm, “Mutual Information Neural Estimation,” in *Proc. Int. Conf. Mach. Learning (ICML)*, Stockholm, Sweden, 2018.
- [14] Z. Aharoni, O. Sabag, and H. H. Permuter, “Computing the Feedback Capacity of Finite State Channels using Reinforcement Learning,” in *Proc. IEEE Int. Symp. Information Theory (ISIT)*, Paris, France, 2019.
- [15] I. Csiszár and J. Körner, *Information Theory: Coding Theorems for Discrete Memoryless Systems*. Academic Press, 1981.
- [16] A. Thangaraj, G. Kramer, and G. Böhcherer, “Capacity Bounds for Discrete-Time, Amplitude-Constrained, Additive White Gaussian Noise Channels,” *IEEE Trans. Inf. Theory*, vol. 63, no. 7, pp. 4172–4182, Jul. 2017.
- [17] F. Topsøe, “An information theoretical identity and a problem involving capacity,” *Studia Sci. Math. Hungarica*, vol. 2, pp. 291–292, 1967.
- [18] J. Kemperman, “On the Shannon capacity of an arbitrary channel,” *Indagationes Math.*, vol. 77, no. 2, pp. 101–115, Jan. 1974.
- [19] A. Lapidoth and S. Moser, “Capacity bounds via duality with applications to multiple-antenna systems on flat-fading channels,” *IEEE Trans. Inf. Theory*, vol. 49, no. 10, pp. 2426–2467, Oct. 2003.
- [20] D. McAllester and K. Stratos, “Formal Limitations on the Measurement of Mutual Information,” in *Proc. Int. Conf. Artificial Intelligence and Statistics (AISTATS)*, virtual, 2020.
- [21] B. Poole, S. Ozair, A. Van Den Oord, A. A. Alemi, and G. Tucker, “On variational bounds of mutual information,” in *Proc. Int. Conf. Mach. Learning (ICML)*, Long Beach, California, 2019.
- [22] D. P. Kingma and J. Ba, “Adam: A Method for Stochastic Optimization,” in *Proc. Int. Conf. Learning Representations (ICLR)*, San Diego, CA, 2015.
- [23] A. McKellips, “Simple tight bounds on capacity for the peak-limited discrete-time channel,” in *Proc. IEEE Int. Symp. Information Theory (ISIT)*, Chicago, IL, 2004.
- [24] A. Lapidoth, S. M. Moser, and M. A. Wigger, “On the Capacity of Free-Space Optical Intensity Channels,” *IEEE Trans. Inf. Theory*, vol. 55, no. 10, pp. 4449–4461, Oct. 2009.
- [25] K. Keykhosravi, G. Durisi, and E. Agrell, “Accuracy Assessment of Nondispersive Optical Perturbative Models through Capacity Analysis,” *Entropy*, vol. 21, no. 8, pp. 1–19, Aug. 2019.
- [26] I. Sason and S. Verdú, “ f -Divergence Inequalities,” *IEEE Trans. Inf. Theory*, vol. 62, no. 11, pp. 5973–6006, Nov. 2016.
- [27] E. Ustinova and V. Lempitsky, “Learning deep embeddings with histogram loss,” in *Proc. Advances in Neural Information Processing Systems (NIPS)*, Barcelona, Spain, 2016.